14

ANALYSIS AND EXPERIMENTS OF POSTBUCKLING BEHAVIOR OF T-SHAPED CFRP STIFFENERS

Takashi Ishikawa, Yoichi Hayashi and Masamichi Matsushima
Airframe Division
National Aerospace Laboratory
Tokyo, JAPAN

1. INTRODUCTION

In the strength design of composite primary aircraft structures, initial buckling prediction and postbuckling behavior description are the major critical factors. The present paper describes a comparison between numerical and experimental results for linear buckling stress and postbuckling behavior of T-shaped carbon fiber/polymer composite (CFRP) stiffeners used commonly in actual aircraft structures. The final goal is to estimate numerically the ultimate strength after buckled state based on rather simple assumptions. The software used here is the commercial level code, NISA-II. Some auxiliary numerical method such as Rayleigh-Ritz method is also used. The tested stiffeners are made of CF/epoxy and CF/PEEK(Poly-Ether-Ether-Ketone). The latter material is a potential candidate for a drastic weight reduction of aircraft structure.

2. BRIEF DESCRIPTION OF COMPRESSION TESTS OF T-STIFFENERS

T-stiffeners made of CFRP were fabricated by Fuji Heavy Industries (FHI) LTD[1]. An overview of the shape and dimension of the specimens is shown in Fig.1. Some comments are given here for better description of the model. The materials used are CF/PEEK (APC-2) and CF/epoxy (P3060). Flange width, b_f, of most specimens is 42mm, referred as N-type. Specimens with some wider flange width referred as W-type are also prepared for CF/epoxy. Web width, b_w, is determined as the following equation so that it exceeds half of b_f slightly. Model length is mostly 140mm and the rest is 280mm.

$$(b_w - t) / \{(b_f - t) /2 \} = 1.09 \qquad 1)$$

Model thickness is well controlled into 2.6 - 2.7mm range in the case of CF/epoxy. For CF/PEEK models, the thickness control was not perfect and it tended to thinner with considerable scatter than the designed thickness because the fabrication was done a few years ago under unmatured know-how. In the present situation, accuracy of the thickness in CF/PEEK components is reaching the level of CF/epoxy. A global warping or distortion of the model was measured for some specimens in order to determine initial imperfection extent.

Stacking sequence used mainly, designated A, is shown in Fig.1 where the total ply number is 20. A few specimens have the other sequence of B with 20 plies, $(45/0^2/-45/0^2/45/0/-45/90)_{sym.}$, in order to examine the effect of D_{16} and D_{26} on initial buckling behavior.

Compression tests were done by a stroke controlled testing machine (Instron 1128). A flat steel compression plate was used without any potting end. For doing that, a precise fitting between the plate and specimen was required through pressure-sensor paper. Crosshead speed used was 0.5mm/min. An examination of the boundary conditions to describe the real situation is one

focussing point of the present paper. A picture of the test for a specimen of 140mm in length is shown in Fig.2. At actual testings, sampled data of a load, two lateral deflections of web and flange centers in terms of the loading direction, and 13 strain gage indications were continuously recorded by a computer data logger at a 200msec. sampling interval.

3. OUTLINE OF NUMERICAL METHODS AND INPUT MATERIAL DATA

The main tool for the numerical calculation was a commercial level finite element code, NISA-II. The used element type was an isoparametric laminate shell element of 4 nodes. This element is capable of consideration of transverse shear deformation. The number of elements was mostly 168, which will be shown indirectly later. The lowest eigenvalue means the buckling load and then buckling stress is obtained. Convergence check told that this subdivision was practically good enough within 1% error of buckling load.

The other tool of calculation is a sort of Rayleigh-Ritz method which was used for a prediction of linear buckling stress at the initial phase of research. The purpose of this method is to examine the effect of D_{16} and D_{26} on initial buckling behavior. However, the detail of description is skipped here.

Regardless of the numerical tools, the assumed elastic moduli of a unidirectional CFRP lamina is crucial for the numerical prediction. For the CF/PEEK material system, verified values in the authors' work[2] are also adopted. For the CF/epoxy material, the estimated moduli based on the author's method[3] are modified corresponding to $V_f = 67\%$. They are summarized in Table 1 where the values of transverse Poisson's ratio which do not provide serious effects might be greater than reality.

4. COMPARISON OF PREDICTION AND EXPERIMENTS FOR LINEAR BUCKLING BEHAVIOR

The first point of discussion is the effect of D_{16} and D_{26} on the linear buckling stress. However, the detail is skipped here except for a brief comment that larger D_{16} reduces the buckling stress.

The second but the most practical point is a dependency of the buckling stress upon the ratio of the flange or web width to its thickness. If fabrication technology of stiffener is not matured enough, flange or web thickness may show some fluctuation. So, such a dependency is considered to be important. Comparison between numerical initial buckling stresses by NISA-II and experimental results are shown in Fig.3. Numerical results are based on the combination of stacking sequence A, fixed loading and supporting edge conditions, and realistic corner radii (R=3mm for CF/epoxy and R=2mm for CF/PEEK). It should be also noted that initial imperfection of the order of 1/100 thickness is included in modelling to keep compatibility with nonlinear analysis stated later, and that Eq.(1) is applied for changing b'_w ($=b_w - t/2$).

Numerical predictions are generally in excellent agreement with experimental results. One crucial point for such good correlation is fixed boundary conditions at the edges. Figure 3 shows that the initial buckling stress rapidly decreases as b'_w/t increases. This finding leads to unintentional loss of buckling stress margin due to slightly less thickness than designes. The experimental results for CF/PEEK indicated by filled legends correspond to some scattered values of b'_w/t which resulted unintentionally because of the unestablished fabrication technique of those days. This point is very important for practical application of CF/PEEK aircraft structures.

The third point of discussion about the initial buckling behavior is an effect of unidirectional filler string inserted at the intersection line of the T-stiffener upon the buckling stress. The amount of this filler can be geometrically related to a corner radius along the line. So, it can be translated as the effect of the corner radius. This problem has been treated in some literature[4],[5]. A target on this research is to find the simplest approach for consideration of this effect. Although the detail is omitted here, it is revealed that the FEM model using the laminate element with UD core material can provide reasonable results and that neglect of this corner radius effect gives considerably poor agreement with experiments.

5. COMPARISON OF NUMERICAL AND EXPERIMENTAL POSTBUCKLING DEFORMATION

The next point of discussion is postbuckling behavior, particularly out-of-plane deformation. Capability of geometrical nonlinear analysis is indispensable for FEM software to obtain this type of solution. Another indispensable factor is to introduce the initial imperfection. An imperfection shape sinusoidal in the x direction and linear in the y direction is assumed where the maximum amplitude is specified as 1/100 of the thickness after the average of measured imperfection amplitudes. The element used and mesh pattern are the same as in the linear solution.

Numerical postbuckling analysis was conducted for the case of W-type CF/epoxy T-stiffener, L=140, b_f=51.0, b''_w=26.5, t=2.54, and R=3 (unit:mm). Two types of loading edge boundary conditions were tried: simply supported and fixed. Two loading modes of displacement controlled (flat compression) and load controlled are also tried in the calculation. Flat compression is modelled so that every node has a common value of displacement in the compression direction. At the first stage, numerical deformation results were compared with experimental deformation shapes. It was found that the agreement was excellent. Next, stress -out-of-plane deflection relations at the center are plotted and compared in Fig.4. The plot of numerical results was done for a 2mm inside point from the edge of the web corresponding to the deflection sensor pickup location. An experimental curve was chosen from the results of four specimens where only a small scatter in data was observed.

Figure 4 indicates first that the results based on the simply supported boundary conditions provide the poorest result plotted by a line with triangles. It can be understood that the fixed condition was almost realized by the flat compression for the present T-stiffener. The load controlled mode (Load Cnt.:dashed line in the Fig.4) apparently provides the best solution. However, load re-distribution after buckling can not be included and axial deformation is different from the flat compression condition in this loading mode. Therefore, this coincidence is regarded merely as "apparently". The most realistic loading mode must be the displacement controlled (Disp. Cnt.:lines with filled and open circles) mode. Thus, some other reason should exist to explain why the numerical prediction curve deviates from the experimental one, particularly at higher stress regions. A convergence check for such a nonlinear portion of behavior was done for cases of a baseline 168 and a fine 672 element and the result was plotted by lines with filled and open circles respectively in Fig.4. Although a slight drop in the stress can be observed by the finer mesh, the tendency of the behavior is considered to be identical. By eliminating some other possibilities, we can reach the following estimation. A most probable reason for the present discrepancy between numerical and experimental postbuckling behavior can presumably be ascribed to material nonlinearity of CF/polymer composites in the fiber direction[2],[6]. Due to this effect, longitudinal elastic modulus of unidirectional CFRP decreases seriously at higher stress. Unfortunately, this effect is not considered in the current analysis. The proof is left for future work.

A similar comparison was done for the case of N-type CF/epoxy T-stiffener, L=140, b''_w=21.6, t=2.66, and R=3 (unit:mm). The indication of the chart is skipped here and it is merely mentioned that prediction coincides well with the experiments.

6. COMPARISON OF NUMERICAL AND EXPERI-MENTAL POSTBUCKLING LOCAL STRAIN AND FINAL FAILURE STRENGTH

After the confirmation of an agreement between the prediction and experiments for lateral deformation, the next interest is the comparison of local strain behavior in the postbuckling range. Experimental back-to-back strain outputs for W-type CF/epoxy at the flange center and 5mm inside from the edge are shown in Fig.5 by solid and solid with bar lines. Numerical predictions are also indicated by circles and triangles. It can be understood that they agree very well. This fact implies the possibility of prediction of the final failure behavior of the present T-stiffeners.

As the final goal of the present research, the final strength prediction was conducted next under three major assumptions. The first is that material strength can be determined as unique values and predicted by a certain failure law in one lamina. The second is that the final failure of the T-stiffener occurs instantaneously when the highest stress at a certain point in a lamina reaches the designated failure law. This assumption implies that no progressive failure is considered here. By AE signal monitoring in the actual tests, this assumption is shown to be rather realistic, particularly for the CF/epoxy pieces. The third assumption is the neglect of a interlaminar stress state near free edges.

Geometrical nonlinear FEM calculations were done for CF/epoxy stiffeners. The assumed failure law is the simplest maximum stress (equivalent to strain) law. Employed baseline strength values are as follows; F_L= 1726MPa, F_L'=1079MPa, F_T=69MPa, F_T'=196MPa, and F_{LT} = 108MPa. Unfortunately, these values were not necessarily obtained through experiments. The active limit for the failure was eventually F_L' for all the calculations. The maximum compressive stress in the fiber direction always reaches this limit at the closest 0° lamina from the back surface of the flange (16th lamina of 20 from the web-intersection surface), or the 16th lamina which is 0° in the web (5th from the back).

In the actual determination of the failure load, linear interpolation of the load steps is required before and after reaching the maximum stress criterion. By repeating such nonlinear calculations and interpolation for various shape parameters, b_f, b''_w, t, and ℓ, we can obtain compressive strength prediction curves for T-stiffeners. Those parameters were varied under the condition of Eq.1). The results are shown in Fig.6 for cases of CF/epoxy L=140 and 280mm. The experimental data around 7 and 9 of $(b_f\text{-}t)/2/t$ values correspond to N and W types, respectively. It can be observed that experimental values for the N type are slightly lower than the prediction and that those for the W type are higher, although the general agreement is rather good. This figure can be regarded as the verification of predictability of the final strength through the present calculation if the failure happens rather instantaneously.

7. CONCLUDING REMARKS

Linear and nonlinear buckling behavior of CFRP T-stiffeners were successfully analyzed by a FEM code. The width to thickness ratio is a very important parameter for good prediction. Corner radius is also important. Longitudinal material nonlinearity of UD-CFRP will provide better agreement in the nonlinear part of the prediction. Final compressive strengths are also predictable.

ACKNOWLEDGMENTS

The authors would like to express their sincere gratitude to those who devoted for a development of difficult fabrication procedures of Carbon/PEEK specimens in Fuji Heavy Industries Co. LTD.

REFERENCES

1. Ishikawa, T., et al., Proceedings of 14th Symposium of Composite Materials, Japan Soc. for Comp. Mater., Kanazawa, Japan, (1989), p.53 (in Japanese).
2. Ishikawa, T., et al., Composite Structures, Vol.23, (1993), p.25.
3. Ishikawa, T., et al., J. Composite Materials, Vol.11, (1977), p.332.
4. Bonanni, D.L., et al., Proceedings of AIAA 29th SDM Conf., Baltimore, MD USA, (1988), p.313.
5. Sambongi, S., Proceedings of 33th JSASS/JSME Structures, Japan Soc. for Aero. Astro. Sci., Yonezawa, Japan, (1989), p.58 (in Japanese).
6. Ishikawa, T., et al., J. Materials Science, Vol.20 (1985), p.4075.

Table 1 Assumed Elastic Moduli of UD-Lamina (unit:GPa)

	E_L	E_T	G_{LT}	ν_L	ν_{TT}
CF/PEEK	117.3	10.30	4.62	0.38	0.5
CF/epoxy	137.0	12.00	5.50	0.34	0.5

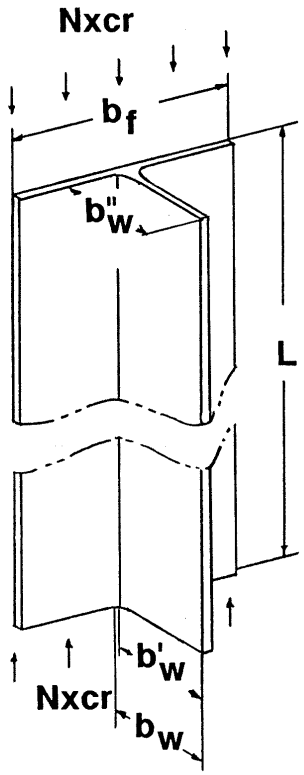

N-Type bf=42

bw=24

L=140
(L=280)

W-Type bf=51

bw=29

L=140

Typical Ply Thickness:

0.118; C/PEEK

0.127;
0.133; C/Epoxy

(unit: mm)

Stacking Sequence:

A: $(45/-45/-45/45/0^3/90/0^2)_{sym.}$

$b'_w=b_w-t/2$ $b''_w=b_w-t$

Figure 1 Shape and Dimensions of T-Shaped Stiffeners

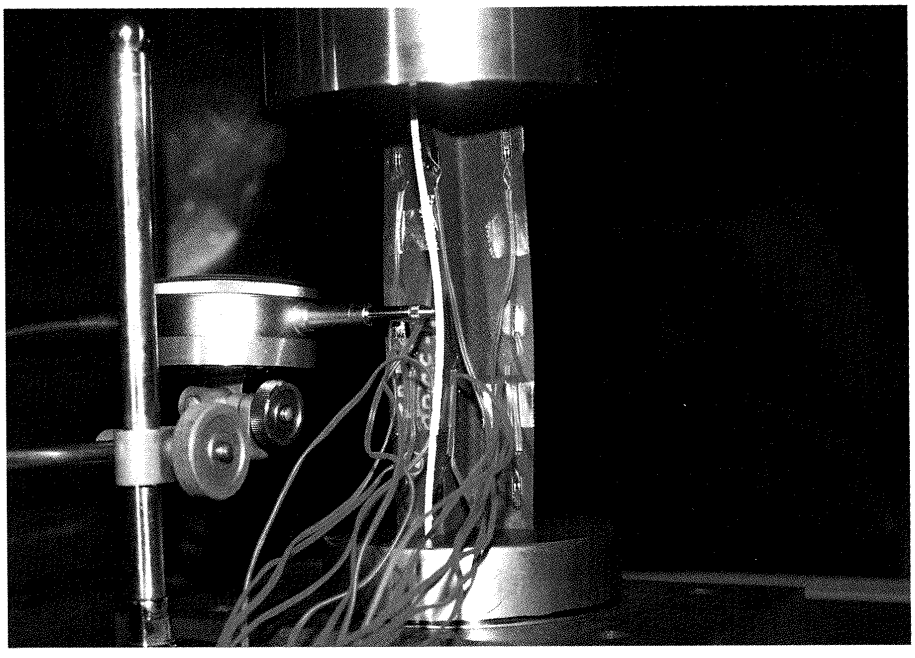

Figure 2 Picture of Compression Test of T-Stiffener

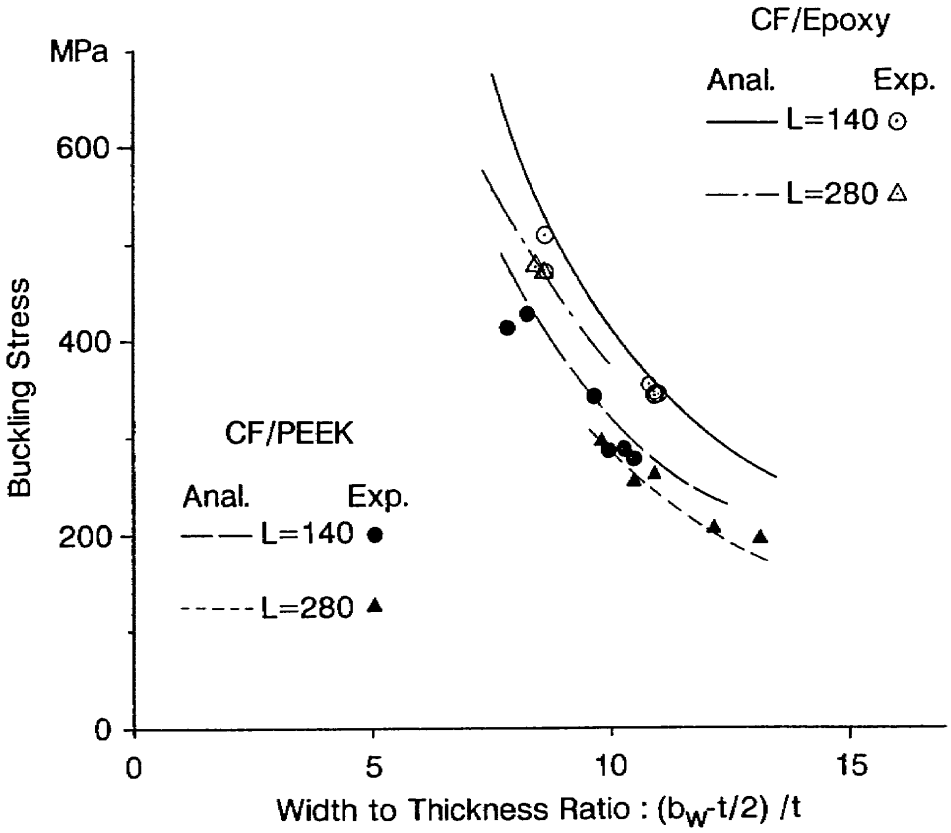

Figure 3 Dependency of Initial Buckling Stress on Width to Thickness Ratio (b'_w / t)

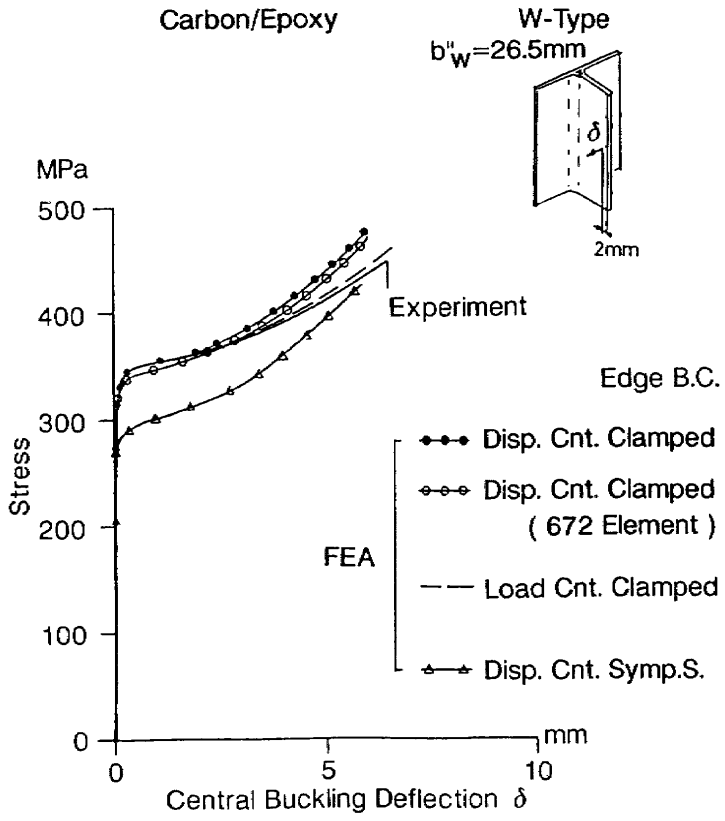

Figure 4 Comparison of Predicted Postbuckling Central Out-of-plane Deflection with Experimental Results for W-Type CF/epoxy Specimen (L = 140mm)

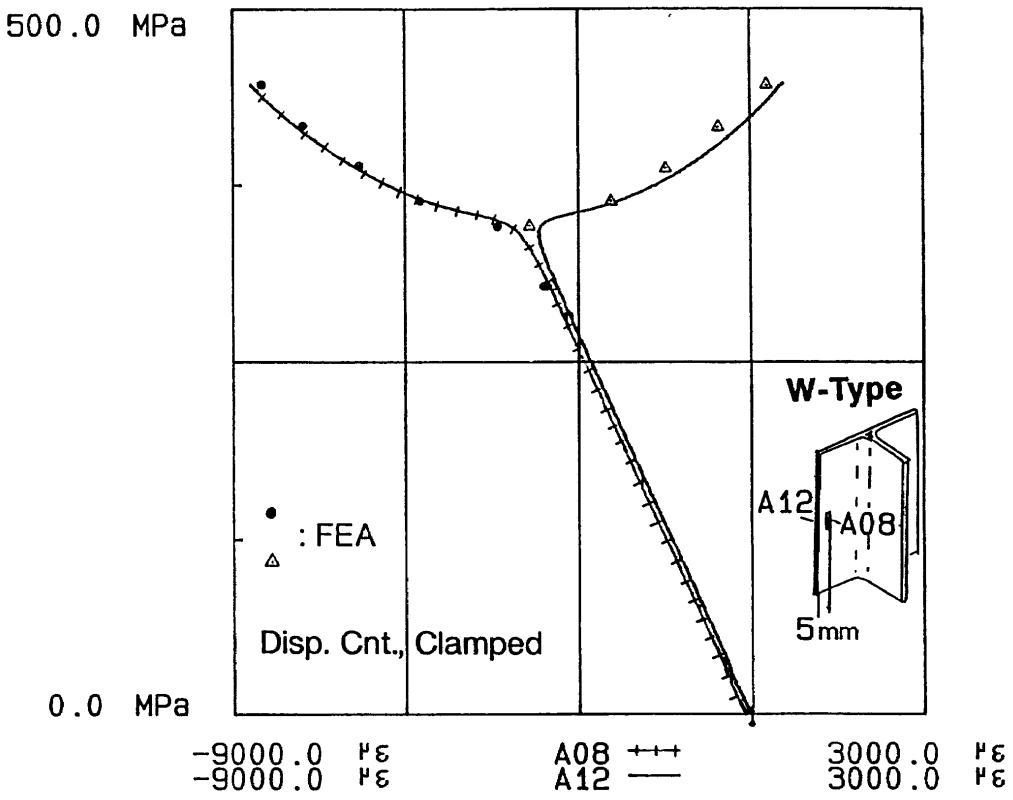

Figure 5 Comparison of Predicted Back-to-back Strain Behavior on Mid-Flange with Experimental Results

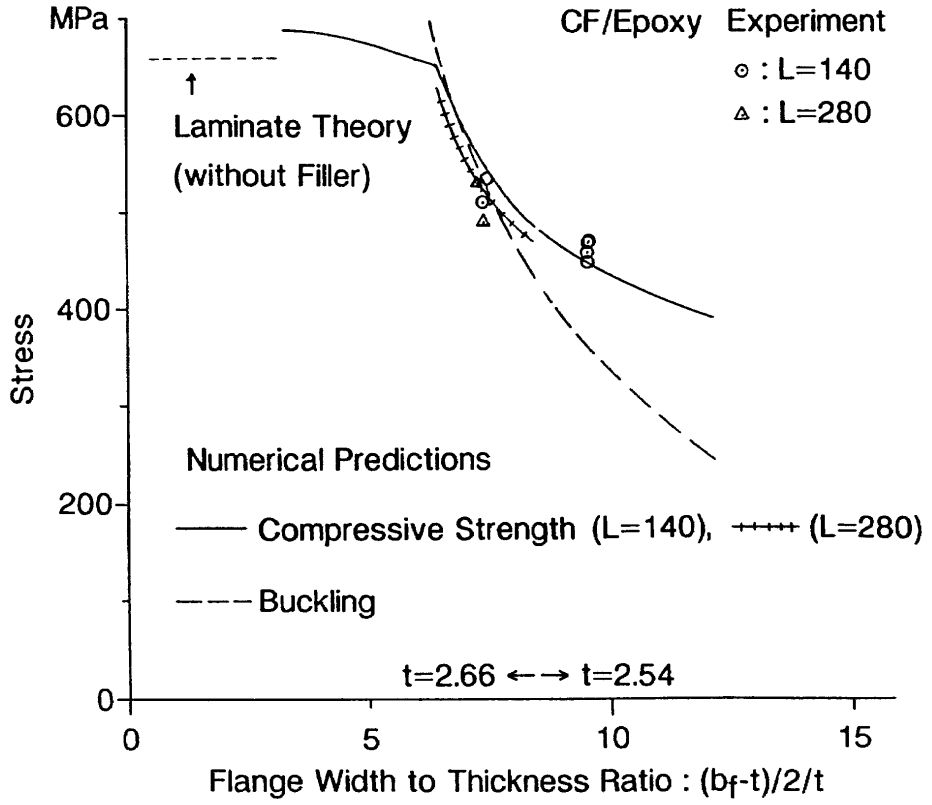

Figure 6 Comparison of Predicted Final Compressive Failure Stress with Experimental Results